Xjenza Online - Journal of The Malta Chamber of Scientists
www.xjenza.org
DOI: 10.7423/XJENZA.2016.1.03

Research Article

Influence of Antimony on Structure and Physical Properties of Molten Tin

Andriy Yakymovych[*1,2], **Stepan Mudry**[2], **Yuriy Plevachuk**[2], **Vasil Sklyarchuk**[2], **Valeri Sidorov**[3]
[1] *University of Vienna, Department of Inorganic Chemistry (Materials Chemistry), Währinger str. 42, 1090 Vienna, Austria*
[2] *Ivan Franko National University Lviv, Department of Metal Physics, Kyrylo and Mephodiy str. 8, 79005 Lviv, Ukraine*
[3] *Ural State Pedagogical University, prosp. Kosmonavtov 26, 620017 Yekaterinburg, Russia*

Abstract. Structure of liquid Sb-Sn alloys were studied by means of viscosity measurements and X-ray diffraction. Structural factors and pair correlation functions were analysed and interpreted using the random atomic distribution model. The features of temperature dependence of the viscosity coefficient were analysed taking into account X-ray diffraction patterns. The results allow us to conclude that Sb atoms substitute for Sn atoms, forming a typical atomic solution, which reveals chemical and topological short-range order. Moreover, certain atoms form Sb- and Sn-based Sb_nSn_m associates and self-associates.

Keywords: liquid alloys, Sb-Sn, viscosity, X-ray diffraction, antimony (Sb), tin (Sn)

1 Introduction

The physical properties of tin (Sn) and antimony (Sb) are similar. Owing to their low melting temperatures, Sn-based alloys can be used in the production of Pb-free solders. In particular, Sb-Sn alloys with other metals are widely used. Therefore, studying Sb-Sn alloys in the liquid state is of great importance.

The equilibrium phase diagram of the Sb-Sn binary system reveals the presence of SbSn and Sb_2Sn_3 metallic phases (Vassiliev, Lelaurain & Hertz, 1997). Measurements of physical properties (Anusionwu, 2006; Zu et al., 2006) and thermodynamic studies (Sommer, Luck, Rupf-Bolz & Predel, 1983) reveal microsegregation in liquid Sb-Sn alloys. Experimental density, surface tension and molar volume differ from the predictions of the regular solution model (Gasior, Moser & Pstrus, 2003). Partial studies on the viscosity and structure of liquid Sb-Sn alloys have also been performed (Sato & Munakata, 1956; Klym, Mudry & Kozyrenko, 1986). The understanding of the relationship between the structure and physical properties is limited and needs further quantitative characterisation. At this point, new experimental studies of dynamic viscosity and the structure of liquid Sb-Sn alloys seem worthwhile.

The phase diagram of Sb-Sn does not reveal unlimited solubility of components, but it indicates the presence of intermediate phases. Therefore, the effects of antimony atoms on the structure of tin are worth studying.

2 Experimental

The samples were prepared in an arc melting furnace filled with argon, from Sb and Sn of high purity (99.99%). The diffraction studies were carried out using a high-temperature diffractometer with a special attachment, which allows investigation of the liquid samples at different temperatures (up to 1800 K). Cu–K_α radiation, monochromatized by means of a LiF single crystal as a monochromator and Bragg–Brentano focusing geometry, were used. The scattered intensity was recorded as a function of the scatering angle within the range $1\,\text{Å}^{-1} < k < 7\,\text{Å}^{-1}$, with an angular step of 0.05° within the region of the principal peak and 0.5° for the remaining values. The scattered intensity was measured with an accuracy of at least 2%. In order to obtain the scattered intensities with such accuracy, the scan time was chosen as 100 s. The diffracted intensity was recorded using a NaI(Tl) scintillator detector together with an amplification system. The sample was placed

Correspondence to: Andriy Yakymovych (yakymovych@online.ua)

in a round cup with 20 mm diameter. Intensity curves were corrected for polarization and incoherent scattering (Cromer & Waber, 1965) and were subsequently normalized to electron units by the Krogh–Moe method (Krogh-Moe, 1956). The obtained intensity curves were used to calculate structure factors (SFs) and pair correlation functions (PCFs). The main structural parameters obtained from SFs and PCFs were subsequently analyzed.

Sb-Sn alloys containing 10, 20, 30 and 40 at.% Sb, respectively, were chosen for viscosity studies. The composition of the samples, weighing about 30 g, was accurate to 0.02 wt%. Each sample was weighed before and after the measurements and no loss of mass was observed. Viscosity measurements were carried out using an oscillating-cup viscometer. The samples were placed in a graphite chamber with internal diameter of 14 mm, filled with helium of high purity and remained there throughout the entire experiment. The temperature was measured with a WRe5/20 thermocouple attached just below the crucible. A detailed description of the equipment was given in Mudry, Sklyarchuk and Yakymovych (2008). Before the measurements were taken, the samples were homogenized for about 5 hours at the highest temperature. The viscosity was measured during the cooling of the samples. The viscosity coefficient η was calculated from the measured logarithmic decrement, whereas the period of the oscillations were determined using the modified Roscoe equation (Vollmann & Riedel, 1996). The viscosity data were obtained with an accuracy of about 3%.

3 Results and Discussion

Experimental structure factors obtained for the liquid $Sb_{100-x}Sn_x$ $(x = 70, 90)$ alloys were compared with those of liquid Sb and Sn near their melting points (5 K above the melting temperature T_m) (Fig. 1). The main structural parameters are listed in Table 1.

The experimental $S(k)$ exhibits a shoulder on the right-hand side of the first peak. This shoulder points to the presence of structural units in which the atoms are covalently bonded.

The positions of the principal peak and the shoulder on the right-hand side of this peak coincide for the liquid $Sb_{10}Sn_{90}$ alloy and liquid Sn (Fig. 1). Upon the addition of 10 at.% of Sb, the second maximum shifted towards lower k values. Upon further increase in the content of antimony, up to 30 at.%, this tendency became more pronounced – the first and second maximum shifted further towards lower k values.

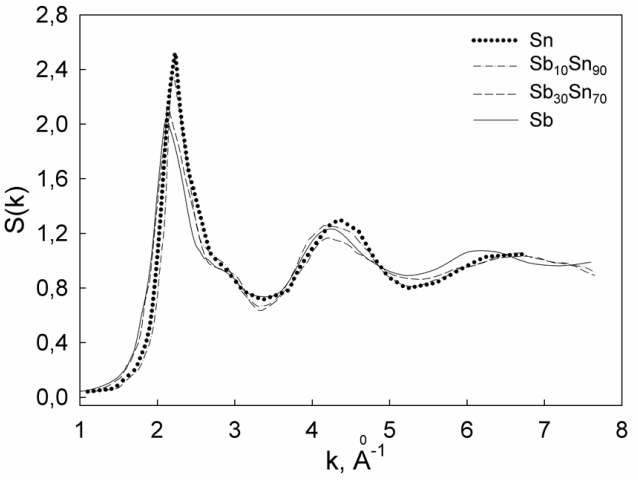

Figure 1: Structure factors of liquid Sb, Sn and liquid $Sb_{30}Sn_{70}$, $Sb_{10}Sn_{90}$ alloys.

By comparing the positions of the maxima (k_1 and k_2) for tin with the structure factors of doped melts, we conclude that Sb atoms added to Sn melt form a structure of their own. For the investigated molten alloys the ratio k_2/k_1 was close to the corresponding ratio of molten tin and molten antimony. The position of the experimental most probable interatomic distance r_1 showed no significant changes with composition. This suggests the presence of associates in the liquid $Sb_{30}Sn_{70}$ alloy, the composition of which is similar to the composition of the investigated melt, as well as the presence of self-associates of Sb_l and Sn_k. This is in agreement with Anusionwu (2006), Zu et al. (2006), Sommer et al. (1983). The experimental coordination number (Z_{exp}) was different from that calculated according to the regular solution model (Z_{RS}) for the liquid alloy at 10 at.% Sb. This was most likely caused by topological disorder-

Table 1: Structural parameters of liquid Sn and Sb-Sn alloys, where k_1 is the position of the first peak of the structure factor; k_2 is the position of the second peak of the structure factor; $S(k_1)$ is the height of the principal peak of the structure factor; r_1 is the experimental most probable interatomic distance; $r_{1(AD)}$ stands for the most probable interatomic distance calculated according to the random atomic distribution model; Z_{exp} is the experimental value of the coordination number; Z_{RS} is the coordination number calculated according to the regular solution model.

at.% Sb	k_1, Å^{-1}	k_2, Å^{-1}	k_2/k_1	$S(k_1)$	r_1, Å	$r_{1(AD)}$, Å	Z_{exp}	Z_{RS}
0	2.23	4.35	1.95	2.52	3.23	3.23	9.7	11.0
10	2.20	4.15	1.89	2.35	3.25	3.24	8.3	7.0
30	2.13	4.20	1.97	2.13	3.20	3.26	7.3	6.9

ing.

The dependence of the coefficient of viscosity on temperature for liquid Sb-Sn alloys with different concentrations is shown in Fig. 2. The experimental curves demonstrate Arrhenius-like behaviour in a wide range of temperatures far from Tm, suggesting that no significant structural changes occur with a change in temperature,

$$\eta = A \exp\left(\frac{E}{RT}\right), \qquad (1)$$

where η is the viscosity coefficient; A is a constant; E is the activation energy; T is the temperature; R is the gas constant.

We also calculated viscosity coefficients using the hard-sphere model (Dymond, 1974). The dependence of viscosity on temperature determined according to this model is compared with experimental data in Fig. 2. The hard-sphere model disagrees with the experimental data, which is most likely caused by the neglect of the attractive force in the formula for the hard-sphere potential (Dymond, 1974)

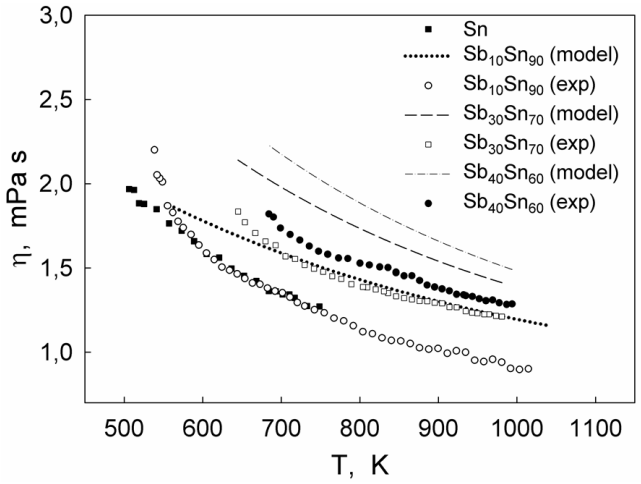

Figure 2: Viscosity of liquid Sn and of liquid Sb-Sn alloys.

The dependence of viscosity on the composition at two temperatures is presented in Fig. 3. Upon the addition of 10 at.% Sb, the viscosity was very similar to that of tin. For alloys containing 30 and 40 at.% of Sb, we noted an increase in viscosity.

Taking into account the profile of the equilibrium phase diagram, the aforementioned behaviour of viscosity was attributed to a structural change which occurred due to the preferential interaction of unlike atoms.

Thus, upon the addition of Sb atoms to tin, the most significant changes were pronounced in the profile of $S(k)$, the peak positions and the coordination number (Fig. 1, Table 1). In particular, $S(k_1)$ decreased and the second maximum shifted towards lower k values. A large discrepancy between the experimental results for

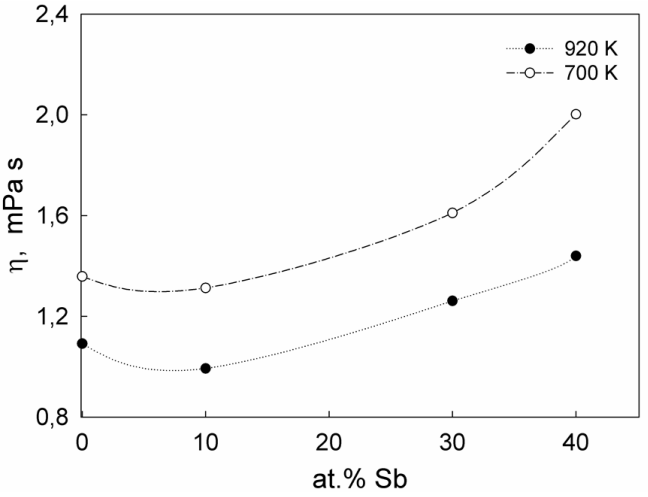

Figure 3: The concentration dependence of viscosity for liquid Sb-Sn alloys.

Z and the calculated results for liquid $Sb_{10}Sn_{90}$ suggests that for low concentrations of Sb in the melts near the melting point we deal with a micro-inhomogeneous structure. Such behaviour is in agreement with viscosity results obtained for liquid $Sb_{10}Sn_{90}$, which revealed a rapid increase in the values in the temperature dependence (Fig. 2) and divergence from Arrhenius-like behaviour (Fig. 4) in the temperature region near T_m.

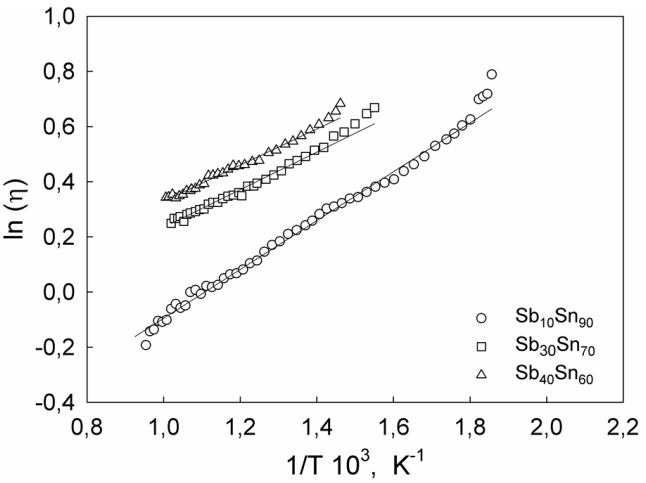

Figure 4: Dependence of viscosity of liquid Sb-Sn alloys on reciprocal temperature.

For higher concentrations of antimony, the interaction between the atoms of Sb and Sn was more pronounced and led to a change in the size of structural units. This was confirmed by an increase in the experimental values for viscosity of liquid Sb-Sn alloys, as compared with the viscosity of liquid Sn (Fig. 2). From this, the presence of associates and self-associates in liquid Sb-Sn alloys is inferred. Our data are in agreement with the res-

ults obtained in Sato and Munakata (1956), Klym et al. (1986).

The addition of a small amount of Sb neither significantly changed the structure (compared to pure Sn) at higher temperatures, nor led to the formation of a micro-inhomogeneous structure in the temperature region near the melting point.

The atomic structure changes upon subsequent addition of Sb atoms. An associated solution is formed, which is accompanied by a decrease in the values of the activation energy (Table 2). This is due to covalent bonding between Sb-Sb and Sn-Sn, which persists in the liquid state.

Table 2: Values of activation energy for liquid Sb-Sn alloys

at.% Sb	10	30	40
E, kJ mol^{-1}	7.37	5.66	5.45

4 Conclusions

Viscosity of liquid Sb-Sn alloys containing 10, 30 and 40 at.% Sb, respectively, increased with an increase in the content of Sb. Such behaviour was caused by the formation of clusters of Sb and their cooperation. The observed structural features and the viscosity of the liquid alloy with 10 at.% Sb suggests that atomic rearrangement occurred in the alloy in the temperature region near the melting point.

References

Anusionwu, B. C. (2006). Thermodynamis and surface properties of Sb-Sn and In-Sn liquid alloys. *Pramana - J. Phys. 67*(2), 319–330.

Cromer, D. T. & Waber, J. T. (1965). Scattering factors computed from relativistic Dirac-Slater wave functions. *Acta Cryst. 18*, 104–109.

Dymond, J. H. (1974). Corrected Enskog theory and the transport coefficients of liquids. *J. Chem. Phys. 60*(3), 969–973.

Gasior, W., Moser, Z. & Pstrus, J. (2003). Surface tension, density, and molar volume of liquid Sb-Sn alloys: Experiment versus modeling. *J. Phas. Equilibria. 24*(6), 504–510.

Klym, N. M., Mudry, S. I. & Kozyrenko, V. N. (1986). Short range order in the liquid Sb-Sn alloys. *Neorg. Mater. 22*(2), 201–203.

Krogh-Moe, J. (1956). A method for converting experimental X-ray intensities to an absolute scale. *Acta Cryst. 9*, 951–953.

Mudry, S., Sklyarchuk, V. & Yakymovych, A. (2008). Influence of doping with Ni on viscosity of liquid Al. *J. Phys. Studies. 12*(1), 1601–1605.

Sato, T. & Munakata, S. (1956). Studies on the viscosity of molten metals and alloys. (III): The density of molten Sb-Sn and Sb-Pb alloys and the viscosity coefficients of molten Sb-Sn, Sb-Pb and Al-Cu alloys. *Bull Res. Inst. Min. Dress. Met. Tohoku Univ. 11*(2), 183–187.

Sommer, F., Luck, R., Rupf-Bolz, N. & Predel, B. (1983). Chemical short range order in liquid Sb-Sn alloys proved with the aid of the dependence of the mixing enthalpies on temperature. *Mat. Res. Bull. 18*, 621–629.

Vassiliev, V., Lelaurain, M. & Hertz, J. (1997). A new proposal for the binary (Sn,Sb) phase diagram and its thermodynamic properties based on a new e.m.f. study. *J. Alloys Comp. 247*, 223–233.

Vollmann, J. & Riedel, D. (1996). The viscosity of liquid Bi-Ga Alloys. *J. Phys.: Condens. Matter. 8*(34), 6175–6184.

Zu, F. Q., Xi, R. R., Shen, Y., Li, X. F., Ding, G. H. & Liu, H. M. (2006). Electrical resistivity of liquid Sn-Sb alloy. *Condens. Matter*, *18*(10), 2817–2823.